Supporting information

Heterogeneous N-terminal Acylation of Retinal Proteins Results from the Retina's Unusual Lipid Metabolism

Grzegorz Bereta, Krzysztof Palczewski

Department of Pharmacology, School of Medicine, Case Western Reserve University, Cleveland, Ohio 44106-4965, USA

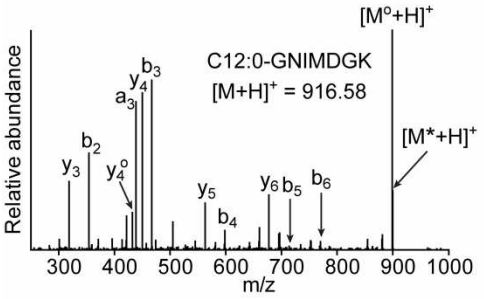

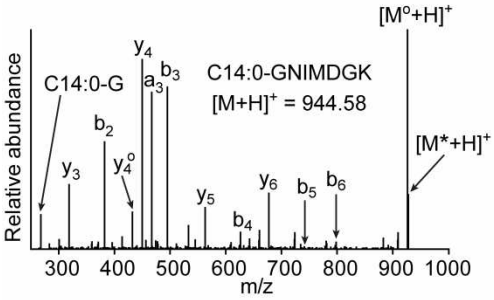

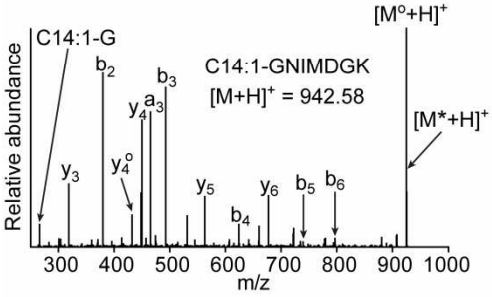

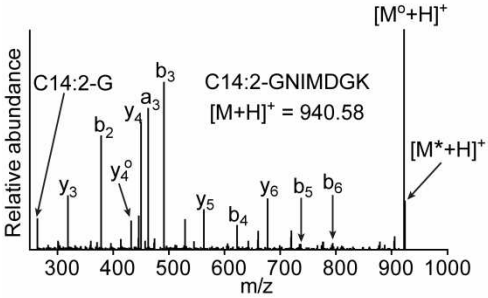

Sequence	Fragment ion	m/z theor.	m/z exper.
C12:0-GN	b_2	354.2	354.2
C12:0-GNI	a_3	439.3	439.2
C12:0-GNI	b_3	467.3	467.2
C12:0-GNIM	b_4	598.4	598.3
C12:0-GNIMD	b_5	713.4	713.3
C12:0-GNIMDG	b_6	770.4	770.2
C12:0-GNIMDGK (-H_2O)	$[M^o+H]^+$	898.5	898.5
C12:0-GNIMDGK (-NH_3)	$[M^*+H]^+$	899.5	899.5
C14:0-G		268.2	268.3
C14:0-GN	b_2	382.3	382.3
C14:0-GNI	a_3	467.4	467.2
C14:0-GNI	b_3	495.4	495.3
C14:0-GNIM	b_4	626.4	626.3
C14:0-GNIMD	b_5	741.4	741.4
C14:0-GNIMDG	b_6	798.4	798.5
C14:0-GNIMDGK (-H_2O)	$[M^o+H]^+$	926.5	926.5
C14:0-GNIMDGK (-NH_3)	$[M^*+H]^+$	927.5	927.6
C14:1-G		266.2	266.3
C14:1-GN	b_2	380.3	380.2
C14:1-GNI	a_3	465.3	465.2
C14:1-GNI	b_3	493.3	493.2
C14:1-GNIM	b_4	624.4	624.3
C14:1-GNIMD	b_5	739.4	739.4
C14:1-GNIMDG	b_6	796.4	796.4
C14:1-GNIMDGK (-H_2O)	$[M^o+H]^+$	924.5	924.5
C14:1-GNIMDGK (-NH_3)	$[M^*+H]^+$	925.5	925.5
C14:2-G		264.2	264.3
C14:2-GN	b_2	378.2	378.2
C14:2-GNI	a_3	463.3	463.2
C14:2-GNI	b_3	491.3	491.3
C14:2-GNIM	b_4	622.4	622.2
C14:2-GNIMD	b_5	737.4	737.3
C14:2-GNIMDG	b_6	794.4	794.4
C14:2-GNIMDGK (-H_2O)	$[M^o+H]^+$	922.5	922.5
C14:2-GNIMDGK (-NH_3)	$[M^*+H]^+$	923.5	923.5
DGK	y_3	319.2	319.3
MDGK	y_4	450.2	450.3
MDGK (-H_2O)	y_4^o	432.2	432.3
IMDGK	y_5	563.3	563.4
NIMDGK	y_6	677.3	677.4

FIGURE S-1: MS/MS spectra of acylated N-terminal peptides from bovine retinal GCAP1. MS/MS spectra are presented in the left panel. The right panel shows sequences and names of detected fragment ions followed by their theoretical and experimental m/z values. The parent ion is denoted by $[M+H]^+$ while superscripts (^{o}) and (*) indicate a neutral loss of water or ammonia, respectively.

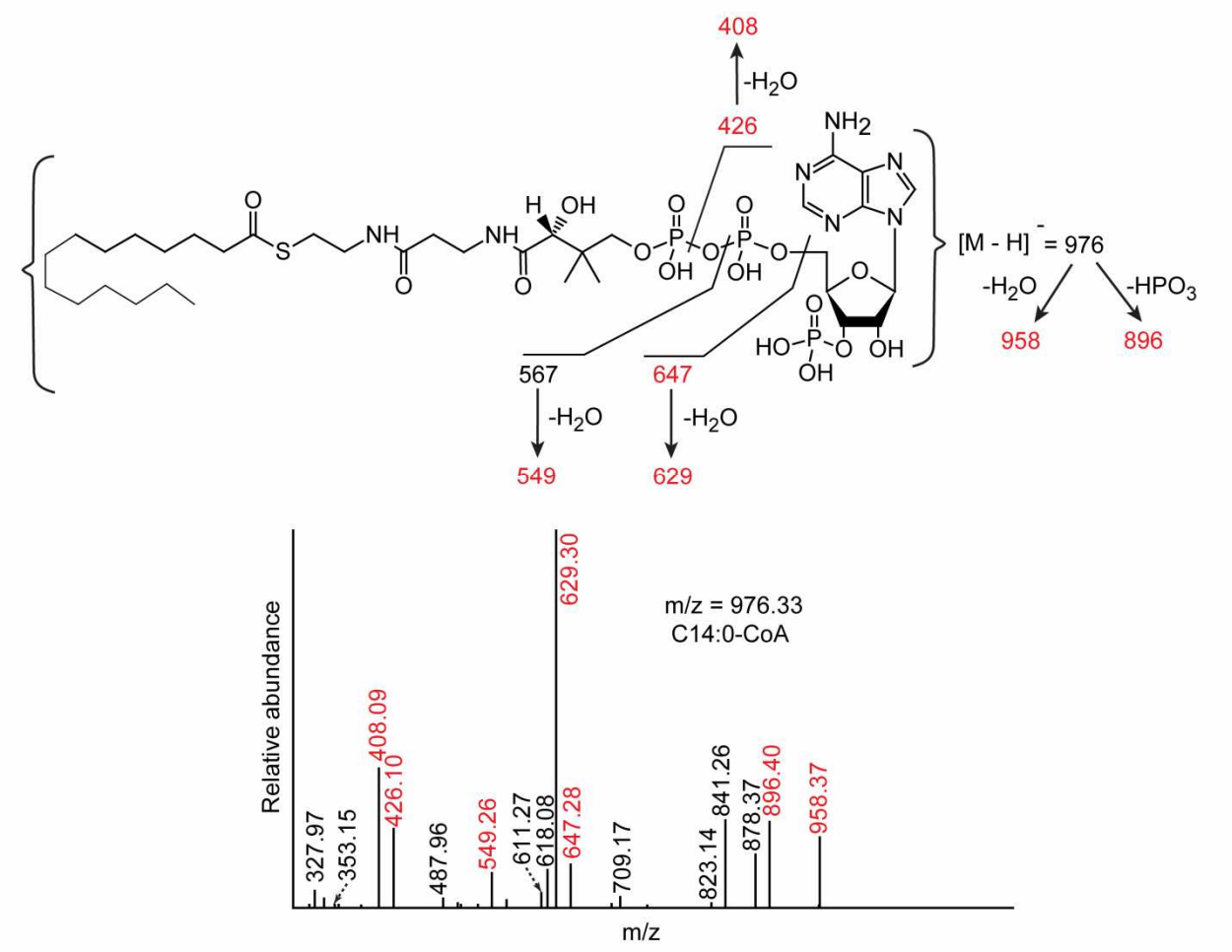

FIGURE S-2. MS/MS fragmentation pattern of C14-CoA. A fragmentation pattern of C14-CoA (upper panel) and its MS/MS spectrum recorded in negative ion mode (lower panel). Peaks with m/z values of 408 and 426 are diagnostic of coenzyme A.

FIGURE S-3. MS/MS spectra of acyl-CoAs purified from bovine retina. These spectra were collected in the negative ion mode. $[M-H]^-$ denotes the parent ion.

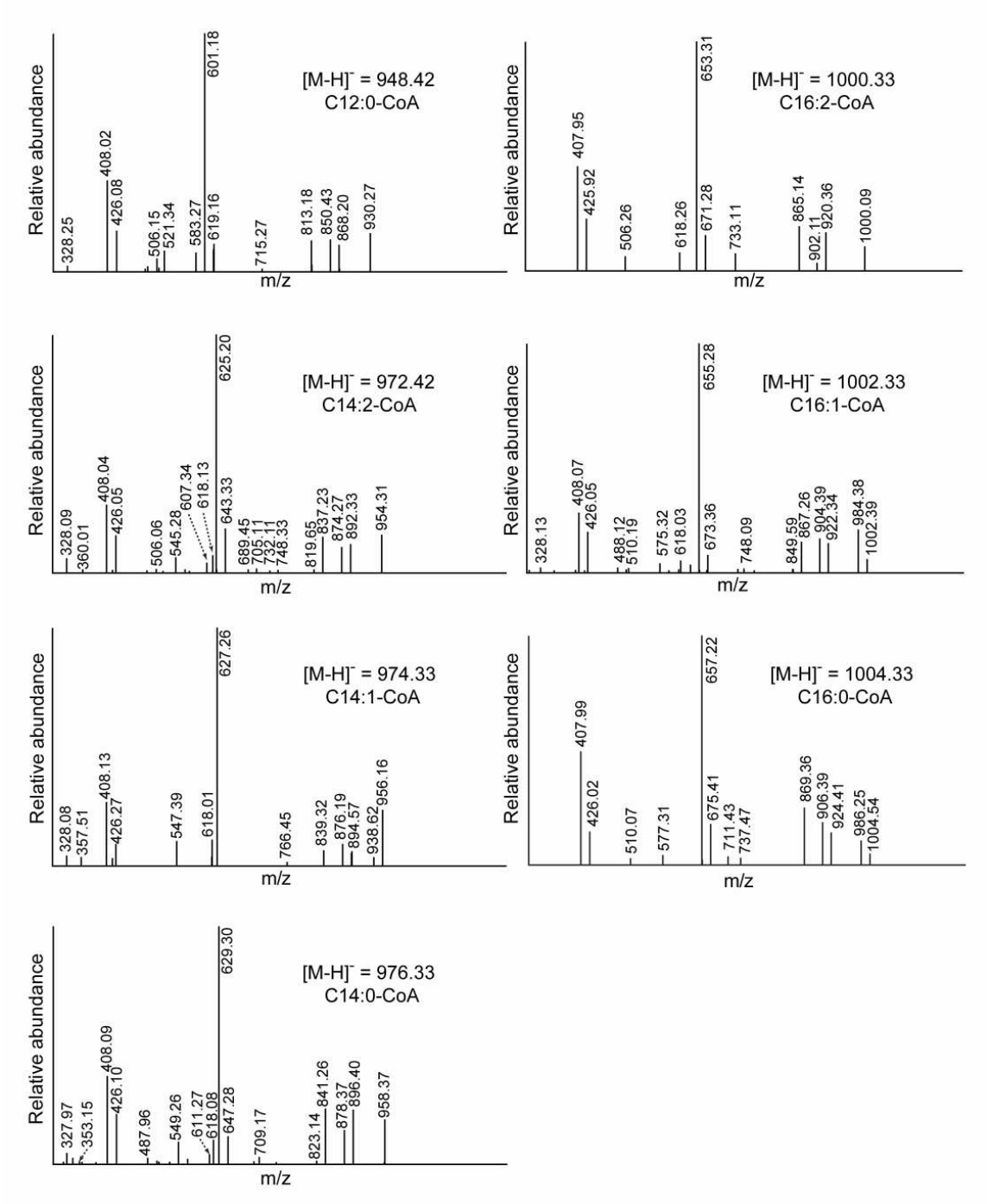

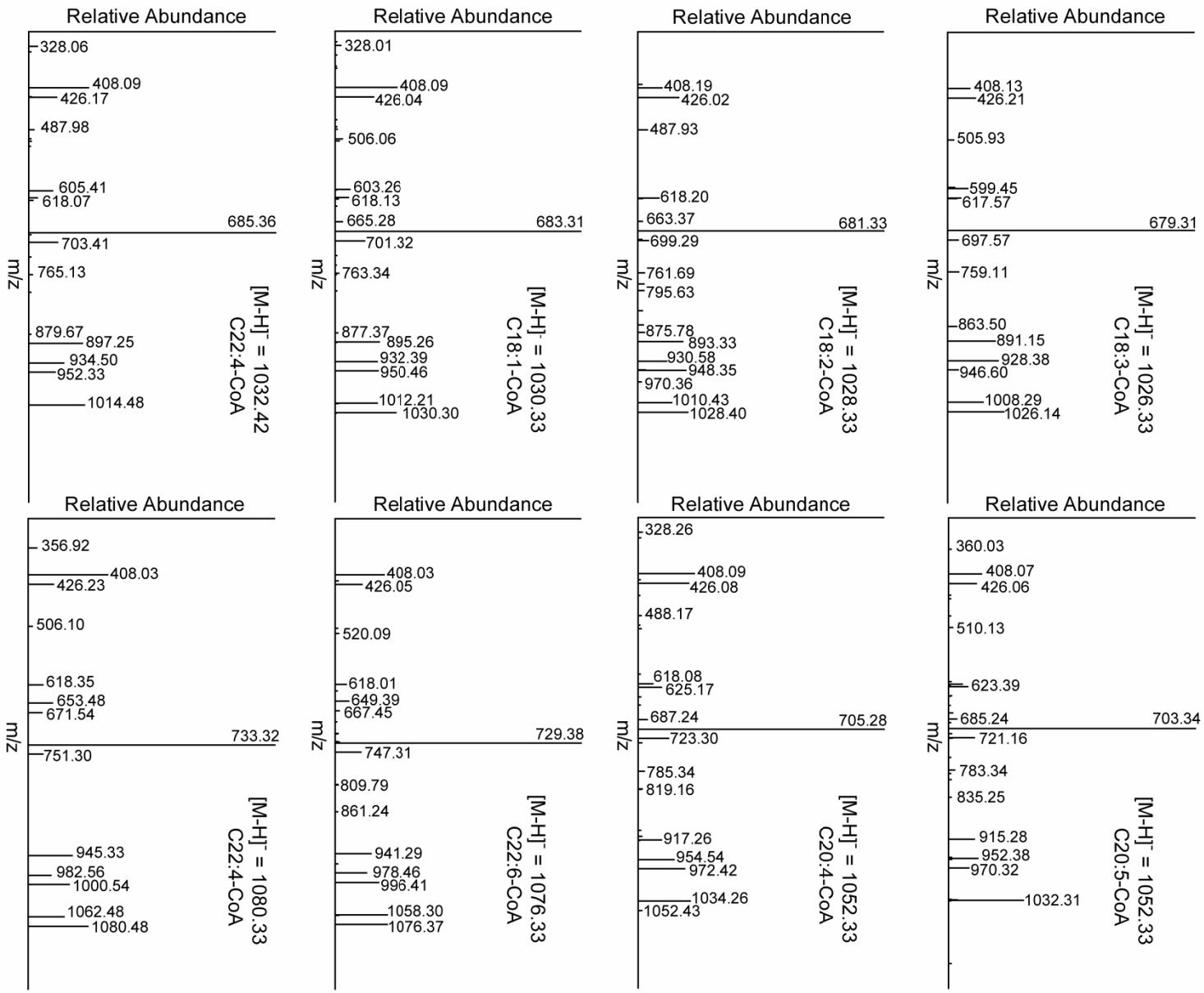
Relative Abundance
m/z
328.06
408.09
426.17
487.98
605.41
618.07
685.36
703.41
765.13
879.67
897.25
934.50
952.33
1014.48
[M-H]- = 1032.42
C22:4-CoA
Relative Abundance
m/z
328.01
408.09
426.04
506.06
603.26
618.13
665.28
683.31
701.32
763.34
877.37
895.26
932.39
950.46
1012.21
1030.30
[M-H]- = 1030.33
C18:1-CoA
Relative Abundance
m/z
408.19
426.02
487.93
618.20
663.37
681.33
699.29
761.69
795.63
875.78
893.33
930.58
948.35
970.36
1010.43
1028.40
[M-H]- = 1028.33
C18:2-CoA
Relative Abundance
m/z
408.13
426.21
505.93
599.45
617.57
679.31
697.57
759.11
863.50
891.15
928.38
946.60
1008.29
1026.14
[M-H]- = 1026.33
C18:3-CoA
Relative Abundance
m/z
356.92
408.03
426.23
506.10
618.35
653.48
671.54
733.32
751.30
945.33
982.56
1000.54
1062.48
1080.48
[M-H]- = 1080.33
C22:4-CoA
Relative Abundance
m/z
408.03
426.05
520.09
618.01
649.39
667.45
729.38
747.31
809.79
861.24
941.29
978.46
996.41
1058.30
1076.37
[M-H]- = 1076.33
C22:6-CoA
Relative Abundance
m/z
328.26
408.09
426.08
488.17
618.08
625.17
687.24
705.28
723.30
785.34
819.16
917.26
954.54
972.42
1034.26
1052.43
[M-H]- = 1052.33
C20:4-CoA
Relative Abundance
m/z
360.03
408.07
426.06
510.13
623.39
685.24
703.34
721.16
783.34
835.25
915.28
952.38
970.32
1032.31
[M-H]- = 1052.33
C20:5-CoA

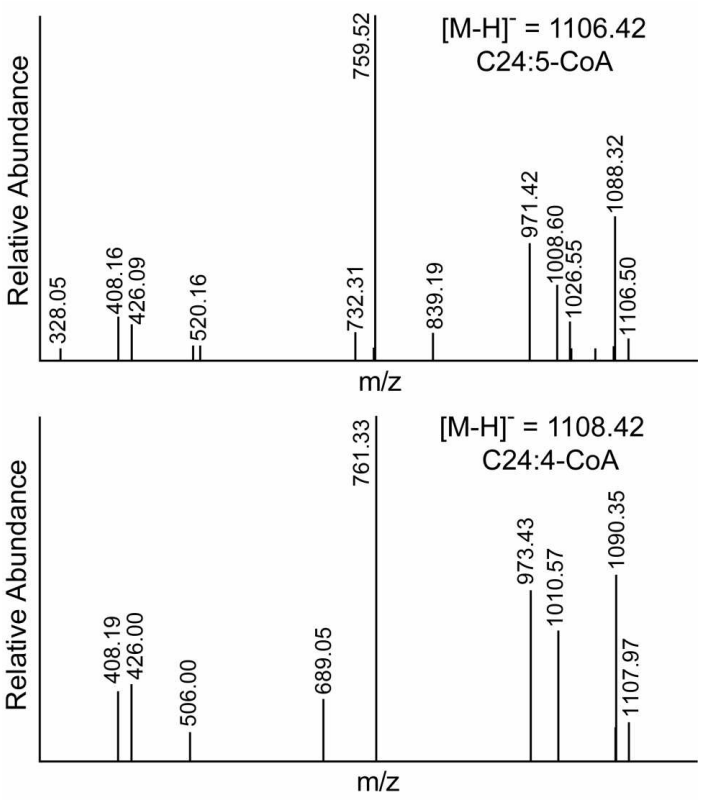
[M-H]- = 1106.42
C24:5-CoA
Relative Abundance
328.05
408.16
426.09
520.16
732.31
759.52
839.19
971.42
1008.60
1026.55
1088.32
1106.50
m/z
[M-H]- = 1108.42
C24:4-CoA
Relative Abundance
408.19
426.00
506.00
689.05
761.33
973.43
1010.57
1090.35
1107.97
m/z

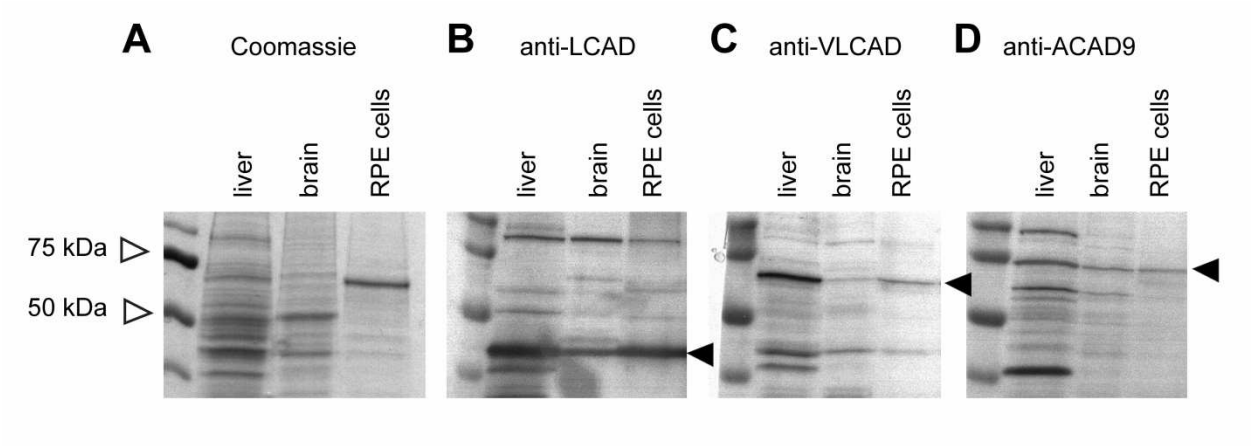

Figure S-4. Expression of LCAD, VLCAD and ACAD9 in mouse liver, mouse brain and mouse RPE cells from ex vivo culture. Coomassie stained gels demonstrate the amount of protein loaded onto each lane (A). Western blots probed with rabbit anti-LCAD, -VLCAD and -ACAD9 antibodies are presented in B, C and D, respectively. Proteins of interest are marked with black arrowheads. Assignment of the ACAD9 band is not unambiguous. These results suggest that LCAD, VLCAD and ACAD9 are present in RPE cells, implying that these cells are not likely to produce high levels of C14:2-CoA and C14:1-CoA. Consequently, production of increased amounts of C14:2-CoA and C14:1-CoA most likely takes place in photoreceptor cells.